

Interdiffusion and Phase Growth Kinetics in Magnesium-Aluminum Binary System

Kaustubh N. Kulkarni and Alan A. Luo

(Submitted October 28, 2012; in revised form December 26, 2012; published online January 31, 2013)

Binary interdiffusion data as functions of composition in the Mg-Al system are essential in modeling kinetics of phase transformations in multicomponent Mg and Al alloys. Interdiffusion and phase growth kinetics were studied in the binary Mg-Al system using multiphase diffusion couples assembled between pure Mg and pure Al at 380, 400 and 420 °C. Two phases, Al_3Mg_2 (β) and $\text{Mg}_{17}\text{Al}_{12}$ (γ) were formed between Al and Mg at the three temperatures studied. Both β and γ phases were observed to follow parabolic growth with time, which suggests that the growth of the two phases is controlled by bulk diffusion mechanisms. The activation energies for the growth of β and γ phases in the temperature range of 380–420 °C were found to be 37.3 ± 4.1 and 187.7 ± 1.9 kJ/mol, respectively. The interdiffusion coefficients were evaluated as functions of compositions in various phases at the three temperatures studied, which were further utilized for evaluating the activation energies and frequency factors for interdiffusion in each phase. The activation energy for interdiffusion in FCC-Al is found to increase with increasing Mg-content whereas the activation energies for interdiffusion in HCP-Mg and γ phases do not vary significantly with composition.

Keywords activation energy, aluminum alloys, Boltzmann/Matano analysis, interdiffusion, magnesium alloys, phase-layer growth kinetics

1. Introduction

Magnesium and aluminum alloys are important materials for vehicle lightweighting due to their lower densities compared with steel. Tremendous amount of work has been reported in the literature on the development of new Al- and Mg-based alloys.^[1–5] However, there is a lack of experimental data on the interdiffusion kinetics in the Mg- and Al-based alloys, especially as function of composition. Such kinetic data are essential in order to understand and control the kinetics of metallurgical processes in these alloys such as casting, heat treatment, and thermomechanical processing. Hence, this work was undertaken to evaluate the interdiffusion kinetics in the Mg-Al binary system using multi-phase diffusion couples.

Interdiffusion studies in the Mg-Al binary system have been reported in the literature.^[6–10] However, all these studies assumed constant interdiffusion coefficient within each phase. Availability of binary interdiffusion coefficients

as functions of compositions is necessary for optimizing mobility parameters in multicomponent Mg-based alloys containing Al as a major alloying element or Al-based alloys with Mg as a major alloying addition. Knowledge of diffusion mobilities as functions of composition is also essential in order to simulate the kinetic processes in a multicomponent system by utilizing a commercially available kinetic software e.g. to list a few are DICTRA^[11] and PAN-Precipitation module of PANDAT.^[12] Hence, in this work, multiphase diffusion couples assembled between pure Mg and pure Al are used to evaluate interdiffusion coefficients as functions of compositions in HCP-Mg and FCC-Al solid solutions. The interdiffusion coefficients and the phase growth kinetics are also evaluated for the two binary intermetallics, $\text{Mg}_{17}\text{Al}_{12}$ (γ) and Al_3Mg_2 (β).

2. Background

The interdiffusion in a binary system can be described by the Fick's law equation^[13]:

$$\tilde{J}_i = -\tilde{D} \frac{\partial C_i}{\partial x}, \quad (\text{Eq 1})$$

where \tilde{J}_i indicates the interdiffusion flux of a component i , \tilde{D} denotes the binary interdiffusion coefficient and $\frac{\partial C_i}{\partial x}$ is the concentration gradient of component i with respect to the distance co-ordinate x . The interdiffusion coefficients are functions of composition and are usually evaluated from infinite or semi-infinite diffusion couple experiments. In such a diffusion couple experiment, the interdiffusion flux \tilde{J}_i can be evaluated at any point x directly from the experimental concentration profiles of the elements by using the following equation^[14]:

Kaustubh N. Kulkarni, India Science Laboratory, General Motors Global R&D, Bangalore 560066, India; and Department of Materials Science and Engineering, Indian Institute of Technology, Kanpur 208016 UP, India; and **Alan A. Luo**, Chemical and Materials Systems Laboratory, General Motors Global R&D, Warren, MI 48090-9055, USA. Contact e-mail: kkaustub@iitk.ac.in.

$$\tilde{J}_i = \frac{1}{2t} \int_{C_i^- \text{ or } C_i^+}^{C_i(x)} (x - x_0) dC_i \quad (\text{Eq 2})$$

where t is the diffusion time in seconds, C_i^- and C_i^+ are the terminal concentrations of component i , and x_0 is the location of the Matano plane i.e. the plane of mass balance. Here, the molar volume is assumed to be constant over the entire diffusion zone. The integral in Eq. 2 can be evaluated easily as appropriate area under the concentration-versus-distance curve of the desired component. For diffusion couples in which the molar volume varies considerably, Eq 2 must be modified^[15] as follows

$$\tilde{J}_i(x^*) = \frac{C_i^- - C_i^+}{2t} \left[Y_i^* \int_{-\infty}^{x_i^*} \frac{(1 - Y_i)}{V_m} dx + (1 - Y_i^*) \int_{x_i^*}^{\infty} \frac{Y_i}{V_m} dx \right], \quad (\text{Eq 3})$$

where the relative concentrations Y_i are defined to be

$$Y_i = \frac{C_i - C_i^+}{C_i^- - C_i^+}, \quad (\text{Eq 4})$$

and V_m is the molar volume. Equation 3 has the advantage of bypassing the need to locate the Matano plane in determining the interdiffusion fluxes. In a multiphase diffusion couple, multiple phases are developed within the diffusion zone and hence molar volume changes considerably within the diffusion zone. However, Eq 2 and 3 can still be applied as long as the interfaces move parabolically with time.^[16,17]

Once the interdiffusion fluxes are determined in a diffusion couple using Eq 2 or 3, the binary interdiffusion coefficients can be calculated at each composition in the diffusion profile based on Eq 1. The interdiffusion coefficients are expressed as Arrhenius equation:

$$\tilde{D} = \tilde{D}_0 \exp\left(\frac{-\tilde{Q}}{RT}\right), \quad (\text{Eq 5})$$

where \tilde{D}_0 and \tilde{Q} are the frequency factor and activation energy for interdiffusion respectively, R is the gas constant and T is the temperature in Kelvin. Equation 5 suggests that the \tilde{D}_0 and \tilde{Q} for interdiffusion can be determined by plotting $\log \tilde{D}$ against $1/T$.

In a multi-phase diffusion couple, the phase growth kinetics can be tracked by carrying out isothermal diffusion couple experiments at various times and in the couple, in which concentration profiles evolve parabolically with time the thickness of a phase (h) can be related to time (t) through a layer growth constant (k) by the simple parabolic relation $h^2 = kt$.^[9,10,18] The layer growth constant further obeys the Arrhenius relationship and hence, with the knowledge of the layer growth constant as function of temperature, the activation energy for the growth of a phase can be evaluated.^[9,10] It should be noted that the simple relation $h^2 = kt$ tends to ignore the incubation time required for the nucleation of a phase before it can start growing. Such

nucleation time maybe considerable, especially at lower temperature, as will be seen later in Results and Discussion. Hence, it is more appropriate to use the relation of the type:

$$h^2 = kt + c \quad (\text{Eq 6})$$

Equation 6 can be employed to estimate the layer growth constant (k) as well as incubation time for the nucleation ($-c/k$) of the phase in a given diffusion couple. One needs at least two isothermal diffusion couple experiments at two different times to accurately determine the layer growth constant along with the incubation time.

The concentration versus distance profiles obtained in the terminal phases of a diffusion couple can also be used to evaluate impurity diffusion coefficients based upon the method proposed by Hall.^[19] According to Hall's method the variable C' is given as

$$C' = \frac{1}{2}(1 + \text{erf}(u)), \quad (\text{Eq 7})$$

where C' is defined as

$$C' = \frac{C_i - C_i^{-\infty}}{C_i^{+\infty} - C_i^{-\infty}} \quad (\text{Eq 8})$$

and the variable u is a linear function of Boltzmann parameter $\lambda = x/\sqrt{t}$ given by $u = h\lambda + \phi$. Thus, the plot of u versus λ is fitted with a straight line whose slope is equal to h and the intercept is ϕ . Once the values of h and ϕ are found, the interdiffusion coefficients can be obtained by the equation:

$$\tilde{D} = \frac{1}{4h^2} + \frac{\phi\sqrt{\pi}}{2h^2} \exp(u^2) C' \quad (\text{Eq 9})$$

It should be noted that Hall's method assumes the constancy of h and ϕ over the region over which the interdiffusion coefficients are evaluated. Looking at Eq 7, it can be seen that h and ϕ are actually functions of \tilde{D} and hence this method maybe prone to errors in the region where \tilde{D} varies with composition. However, in the terminal alloy of a diffusion couple, if the concentration is diminishing slowly, characterized by a long tail of the concentration profile, impurity diffusion coefficients can be determined as:

$$D_i^* = \lim_{C_i \rightarrow 0} \tilde{D} = 1/4h^2 \quad (\text{Eq 10})$$

3. Experimental Work

Diffusion couples were prepared from pure Mg and pure Al metals, which had been cold rolled (5-15%) and annealed for 7 days at 400 °C in an evacuated quartz tube for producing equi-axed grains. From the annealed Al and Mg, blocks of 7 mm×7 mm×5 mm were prepared. Diffusion couples were prepared by clamping together an Al and a Mg block in a stainless steel jig. In order to ensure perfect contact between the Al and Mg, the two surfaces in contact were metallographically polished to 0.05 μm alumina finish.

The clamped assembly was then sealed in an evacuated quartz tube to avoid exposure to oxygen during diffusion annealing. The quartz tube was evacuated and purged with Ar three times before finally sealing it with the inside pressure of about 10^{-3} torr. The diffusion couples were then annealed at the desired temperature in a tube furnace with the temperature control of ± 1 °C. The temperature of the sample was continuously monitored with the help of an external thermocouple and it was observed that the re-stabilization of the set temperature was achieved within 10-15 min after placing the sample inside the preheated and stabilized furnace. Hence, the reported annealing time was started 15 min after placing the sample inside the furnace. After the diffusion annealing, the diffusion couple was quenched from the annealing temperature into hot water (at about 60-70 °C) in order to retain the high temperature structure and composition profiles. The hot water quench was employed to minimize the cracking of the intermetallic layers formed in the diffusion zone during quenching. The time spent in removing the sealed sample from the furnace and quenching it in water was less than 30 s. The various diffusion couples assembled in this study along with time and temperature of diffusion annealing are listed in Table 1.

The annealed diffusion couples were sectioned parallel to the direction of diffusion and metallographically prepared for the observation of various phases developed in the diffusion zone. The average layer thicknesses of the β and γ phases developed in each diffusion couple were determined under an optical microscope by measuring the thickness at least at twenty different locations. Couples 3, 5 and 8 (see Table 1) were selected for further analysis of interdiffusion coefficients. The concentration profiles developed in these couples were determined by point-by-point analysis with a JEOL JXA-8530F Electron Probe Micro-Analyzer (EPMA) using pure Al and pure Mg standards. The total of the weight percentages sometimes varied between 98 and 102% possibly because of the matrix effects; especially in the intermetallic phases. The EDS and WDS analyses carried out on the same composition planes agreed well for the Al-concentration values. Hence, only the Al intensities measured by WDS were used for the determination of Al-concentration and balance was assumed to be Mg-concentration. Based on the multiple analyses carried out at same composition planes in different phases, the uncertainties estimated in the measured concentrations are less than 0.5%. This is not expected to give rise to significant errors in the calculation of the binary interdiffusion coefficients since concentration gradients are more critical for the calculation of the interdiffusion coefficients rather than the absolute concentrations.

Table 1 Mg-Al binary diffusion couples studied

S.no.:	1	2	3	4	5	6	7	8	9
Diffusion time, h	24	50	91	24	50	94	24	50	94
Diffusion annealing temperature, °C	380			400			420		

4. Results

The micrographs of the diffusion couples annealed at 380, 400 and 420 °C for 24, 24 and 50 h respectively are presented in Fig. 1(a-c). It can be seen from Fig. 1 that two intermediate layers are formed between Al and Mg at all three temperatures studied. EDAX analysis confirmed that these two layers are Al_3Mg_2 (β) and $\text{Mg}_{17}\text{Al}_{12}$ (γ). Binary phase diagram of Al/Mg as assessed by Murray^[20,21] is presented in Fig. 2, in which the dashed lines indicate the tie lines for the three diffusion couple temperatures. The phase diagram suggests that the two intermetallic phases existing between Al and Mg at 380, 400 and 420 °C are Al_3Mg_2 (β) and $\text{Mg}_{17}\text{Al}_{12}$ (γ). Thus, the formation of the two intermediate phases in the Mg/Al diffusion couples studied is in accordance with the equilibrium phase diagram established by Murray. Also, the planar interfaces observed in all the diffusion couples imply local equilibrium at the interfaces and makes the multiphase couples suitable for interdiffusion analysis.

4.1 Phase Growth Kinetics

In Fig. 3, the square of the measured layer width (h^2) is plotted against time (t) for both β and γ phases for the three temperatures studied. The error bars on the data-points in Fig. 3 are small and are contained within the symbols. The measurements of time were done within the accuracy of ± 2 s. Since, the annealing times are in days, the uncertainties in the time measurements are not significant. As far as the incubation times are considered, the estimated values from the plots in Fig. 3 should be the minimum estimates with uncertainty of +5 min coming from time required for temperature re-stabilization and from the time spent in removing the sample and quenching in water.

The plots in Fig. 3 show a linear relationship between h^2 and t ; which suggests that the growth of the β and γ phases is controlled by diffusion mechanisms. The plots in Fig. 3 were used to determine the layer growth constant (k) and the incubation time for the β and γ phases based on Eq 6. The layer growth constants and incubation times determined for β and γ at the three different temperatures are presented in Table 2. It can be seen from Table 2 that the layer growth constants for β phase is larger than that for γ phase at all temperatures; about an order of magnitude larger at 380 and 400 °C and more than 3 times larger at 420 °C. On the other hand, the β phase is characterized by much longer incubation times than γ phase at 380 and 400 °C. At 380 °C, the incubation time for β is about 4 h whereas that for γ is just above 1 h. At 420 °C, the incubation times of both the phases are very small; 1 and 6 min for β and γ respectively.

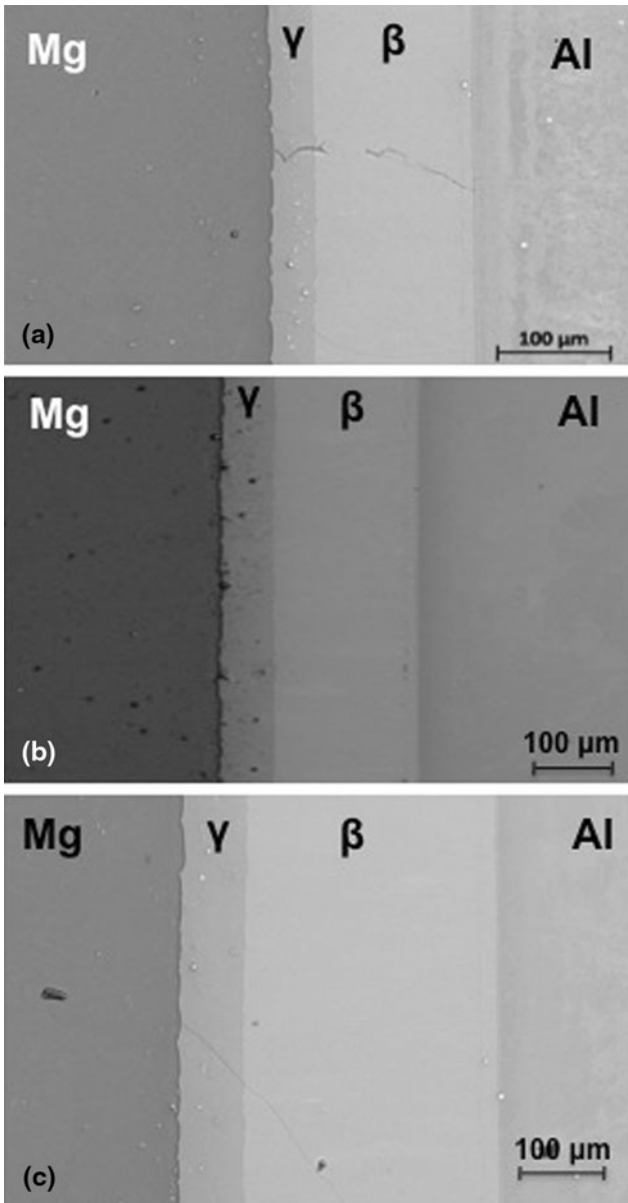


Fig. 1 BSE micrographs of the diffusion zone developed in the Mg/Al diffusion couples annealed at (a) 380 °C for 24 h (b) 400 °C for 24 h and (c) 420 °C for 50 h

The plots of $\ln k$ against $1/T$ are presented in Fig. 4 and are further utilized to estimate the activation energies for the growth of β and γ phases based on the Arrhenius relation. The activation energies and frequency factors so determined for the growth of β and γ are listed in Table 3. The β phase has significantly smaller activation energy for growth than the γ phase.

4.2 Analysis of Interdiffusion Coefficients

The experimental concentration profiles determined by EPMA for the three diffusion couples were analyzed for interdiffusion coefficients using the *MultiDiflux* program.^[22] This program fits the experimental concentration profiles of a multicomponent diffusion couple by least square method

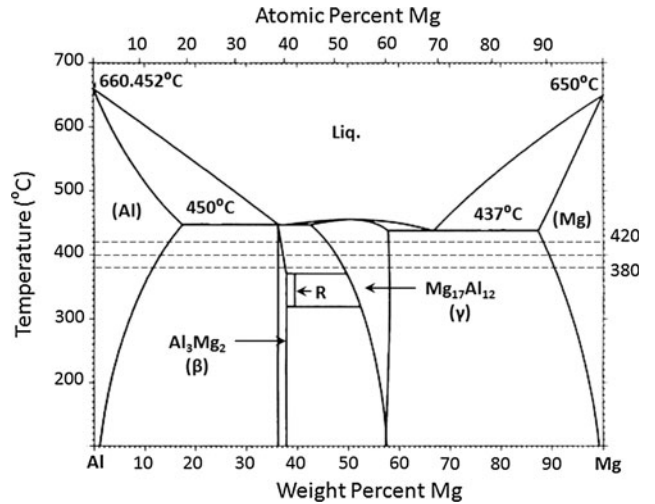


Fig. 2 Al-Mg binary phase diagram.^[20,21] The dashed lines indicate the temperatures at which the diffusion couple experiments were carried out in the present study

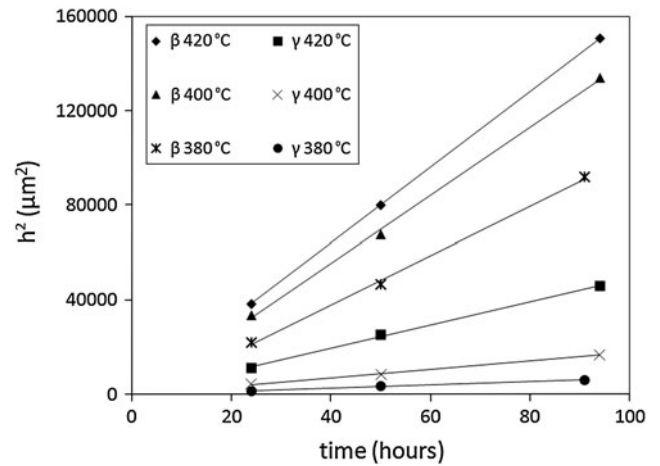
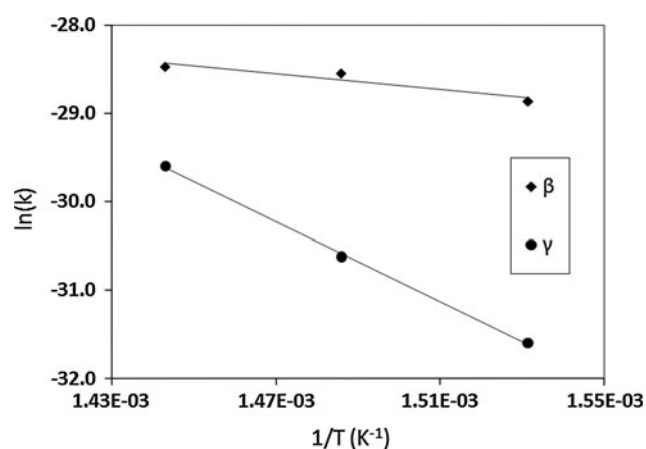


Fig. 3 Growth of β and γ phase layers in Mg/Al diffusion couples at various temperatures and times

using cubic Hermite interpolation polynomials. For a multiphase diffusion couple, the program can be used to fit the profiles in individual phases based on the number and positions of interfaces selected by user. The program also extrapolates the concentrations at the interfaces in each phase. The fitted concentration profiles are then used by the program to evaluate the interdiffusion fluxes and interdiffusion coefficients over the regions selected by user. The experimental as well as fitted concentration profiles and calculated interdiffusion flux profiles are presented in Fig. 5, 6, 7 for the diffusion couples annealed at 380 °C for 91 h, 400 °C for 50 h and 420 °C for 50 h, respectively. As can be seen from Fig. 5(a), 6(a) and 7(a), the concentration profiles within the β phase are close to linear and hence, straight line fitting was assumed for the purpose of fitting and calculating interdiffusion coefficients within the β phase. The profiles in the other phases, however, were fitted with the cubic Hermite

Table 2 Layer growth kinetics for β and γ phases at various times and temperatures

No.	T (°C)	Time, h	Al_3Mg_2 (β) phase			$\text{Mg}_{17}\text{Al}_{12}$ (γ) phase		
			Layer width, μm	Growth constant, m^2/s	Incubation time, min	Layer width, μm	Growth constant, m^2/s	Incubation time, min
1	380	24	148 \pm 1	2.9×10^{-13}	241	39 \pm 1	1.9×10^{-14}	71
2		50	216 \pm 5			58 \pm 2		
3		91	303 \pm 7			78 \pm 3		
4	400	24	183 \pm 2	4×10^{-13}	95	67 \pm 2	5×10^{-14}	51
5		50	260 \pm 3			91 \pm 2		
6		94	366 \pm 3			130 \pm 2		
7	420	24	196 \pm 2	4.5×10^{-13}	1	106 \pm 2	1.4×10^{-13}	6
8		50	283 \pm 1			159 \pm 3		
9		94	388 \pm 3			214 \pm 3		

**Fig. 4** $\ln(k)$ vs. $(1/T)$ plots for the β and γ phase growth. Here, k is in m^2/s and T is in Kelvin**Table 3** Activation energies and frequency factors determined for growth of β and γ phases in the Mg/Al diffusion couples

Al_3Mg_2 (β) phase		$\text{Mg}_{17}\text{Al}_{12}$ (γ) phase	
Activation energy, kJ/mol	k_0 , m^2/s	Activation energy, kJ/mol	k_0 , m^2/s
37.3 \pm 4.1	$2.9 (\pm 0.3) \times 10^{-10}$	187.7 \pm 1.9	19 (± 0.2)

polynomials. The interdiffusion fluxes presented in Fig. 5(b), 6(b) and 7(b) were calculated by the *MultiDiflux* program based on Eq 3 and molar volumes were assumed to be constant over the entire diffusion zone for these calculations. The assumption of molar volumes is expected to give negligible errors in the calculations of the interdiffusion fluxes since the Matano planes calculated for individual elements, Al and Mg, differed by less than 2% of the entire width of the diffusion zone. Although the evaluation of Matano plane helped to confirm that the assumption of

constant molar volumes is valid, it should be noted that the application of Eq 3 for calculation of interdiffusion fluxes does not require the knowledge of the Matano plane and hence minimizes the experimental errors related to the determination of the Matano plane.

The evaluated interdiffusion flux profiles and concentration gradients were used for calculation of interdiffusion coefficients based on Eq 1. The calculated interdiffusion coefficients as functions of compositions in HCP-Mg, FCC-Al and γ - $\text{Mg}_{17}\text{Al}_{12}$ phases at the three different temperatures studied are presented in Fig. 8(a-c). It should be noted that the flattening of concentration profiles of Mg and Al near the terminal alloys present large errors in calculations of concentration gradients and thereby in interdiffusion coefficients. Hence, the interdiffusion coefficients are not reported for the low concentrations of solutes (less than 1 at.% Al in HCP-Mg and less than 2 at.% Mg in FCC-Al). The interdiffusion coefficients evaluated in the three phases are summarized in Tables 4, 5, 6. On account of very narrow range of composition for the β phase at higher temperatures, only average interdiffusion coefficients are calculated for the β phase at each temperature and they are reported in Table 7. The errors in the calculation of interdiffusion coefficients are mainly on account of errors in the evaluation of integrals and concentration gradients from the fitted concentration profiles. The integral calculations for fluxes are done by the *MultiDiflux* program with about 0.1% errors. However, the errors in the determination of concentration gradients are larger especially in the regions of small gradients. Thus, the errors estimated in the calculation of interdiffusion coefficients in most of the regions of the diffusion couples are about 10%. However, in the regions of small gradients, i.e. towards the ends of the couple and within the Al_3Mg_2 phase, maximum errors of 40% are estimated.

The interdiffusion coefficients are then used to calculate the activation energies and frequency factors for interdiffusion in various phases based on Eq 5 and they are also summarized in Tables 4, 5, 6, 7.

4.3 Impurity Diffusion Coefficients

Impurity diffusion coefficient of Mg in FCC-Al (${}^{\text{fcc-Al}}D_{\text{Mg}}^*$) has been evaluated based on Hall's method.

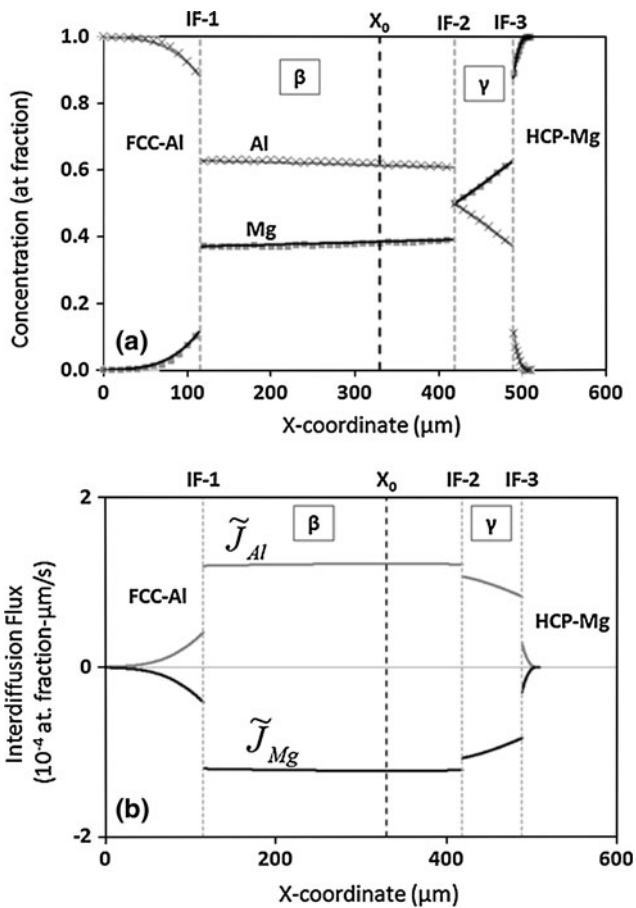


Fig. 5 (a) Concentration profiles and (b) Interdiffusion flux profiles for the Mg/Al diffusion couple annealed at 380 °C for 91 h. The Matano plane is indicated by X_0 and the three interfaces are indicated by IF-1 to IF-3

The plots of u versus λ for FCC-Al obtained from concentration profiles at three different temperatures are presented in Fig. 9(a). Note that x -axis in Fig. 9(a) represents λ for 400 and 420 °C data, and $-\lambda$ for 380 °C data. ${}^{fcc-Al}D_{Mg}^*$ determined based on values obtained from Fig. 9(a) and Eq 10 are presented in Fig. 9(b). The values of activation energies and pre-exponential constants for ${}^{fcc-Al}D_{Mg}^*$ are presented in Table 8 along with the other experimental data available in literature.^[23,24] It is clear from Fig. 5, 6, 7 that Al-profiles inside HCP-Mg are not characterized by a long tail required for accuracy of Hall's analysis as discussed in earlier section. Hence, the Hall's analysis has not been applied in the HCP-Mg region.

5. Discussion

5.1 Phases and Their Growth Kinetics

There have been several studies reported in the literature on the assessment of phase equilibria in the Mg-Al binary system^[20,25,26] and there is a general agreement on the

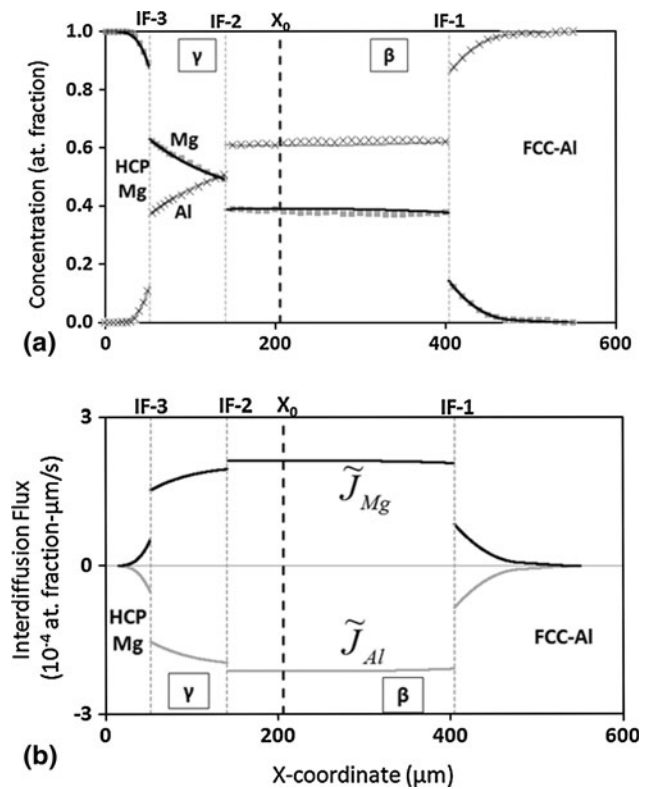


Fig. 6 (a) Concentration profiles and (b) Interdiffusion flux profiles for the Mg/Al diffusion couple annealed at 400 °C for 50 h. The Matano plane is indicated by X_0 and the three interfaces are indicated by IF-1 to IF-3

existence of β and γ phases between Al and Mg. However, in the region between 40 and 60 at.% Mg, there is a debate especially about the temperature range for the existence of ε or R phase. As per the phase diagram assessed by Murray^[20] (shown in Fig. 2), the ε phase exists between 320 and 370 °C and only two intermetallic phases (β and γ) are present above 370 °C. The phase diagram calculated by Zuo and Chang^[25] predicts the existence of ε and ζ phases in the temperature range between 400 and 450 °C. The annealing experiments carried out by Su et al.^[26] on the Mg-Al alloys within this composition range have reported the presence of ε phase only up to 380 °C. Their reported samples annealed at 400 and 425 °C indicated the presence of only β and γ phases at these temperatures. There have been three studies found in the literature on diffusion couples assembled between pure Al and pure Mg.^[6,9,10] Clark and Rhines^[6] detected presence of β, ε and γ phases in the sole diffusion couple assembled at 335 °C. The other two studies have not found any extra phase layer between β and γ in the temperature range of 370-425 °C. The present study also confirms the existence of only two intermetallic phases (β and γ) forming at 380-420 °C in the diffusion couples assembled between pure Mg and pure Al.

Conventionally, the kinetics of growth of a phase developed in a multiphase diffusion couple are described by evaluating the layer growth constant (k) and determining the empirical energy of activation by plotting $\log k$ against

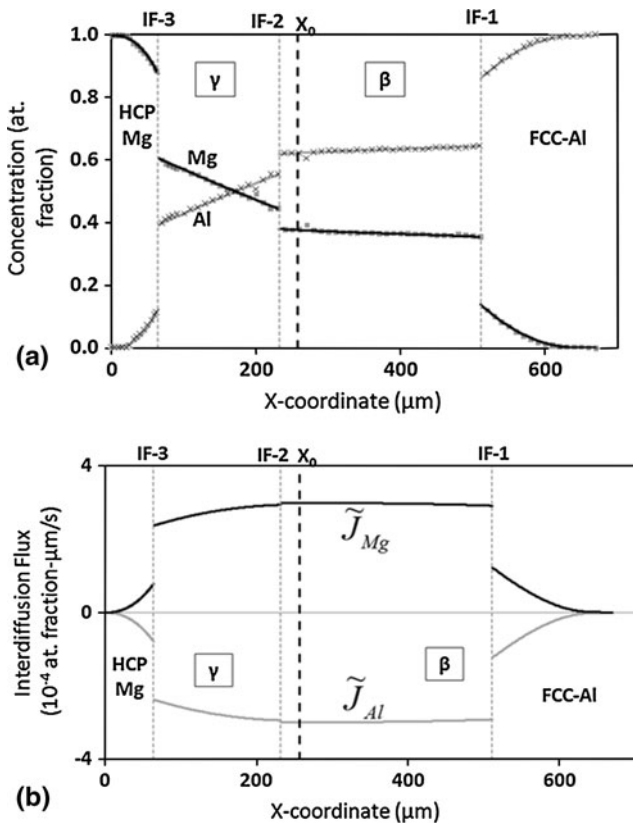


Fig. 7 (a) Concentration profiles and (b) Interdiffusion flux profiles for the Mg/Al diffusion couple annealed at 420 °C for 50 h. The Matano plane is indicated by X_0 and the three interfaces are indicated by IF-1 to IF-3

(1/T). According to Sisson and Dayananda,^[27] the growth rate of a phase-layer in a diffusion couple depends upon the interdiffusion fluxes not only within the phase itself but also in the adjacent phases. For a multiphase couple, characterized by parabolic growth of phases, (for example, consider the β phase in the present study) the rate of the phase growth can be expressed as^[17]:

$$\frac{dh_{\beta}}{dt} = \left[\frac{\tilde{J}_i^{Al} - \tilde{J}_i^{\beta}}{C_i^{Al} - C_i^{\beta}} \right]_{\text{at Al}/\beta \text{ interface}} - \left[\frac{\tilde{J}_i^{\gamma} - \tilde{J}_i^{\beta}}{C_i^{\gamma} - C_i^{\beta}} \right]_{\text{at } \beta/\gamma \text{ interface}}, \quad (\text{Eq 11})$$

where \tilde{J}_i^{Al} , \tilde{J}_i^{β} and \tilde{J}_i^{γ} represent the interdiffusion fluxes of component i in the Al, β and γ phases respectively whereas, C_i^{Al} , C_i^{β} and C_i^{γ} represent the concentrations in these phases. h_{β} is the layer thickness of β phase at a time t . The term in the first bracket on right hand side of Eq 11 is the interface velocity of Al/ β interface whereas the term in the second bracket represents the interface velocity of the β / γ interface. Thus, the rate of layer growth of β phase and the activation energies of growth so determined depend on the interdiffusion coefficients in FCC-Al, β and γ phases. Similarly, the activation energy for the growth of γ phase is dependent on

the interdiffusion coefficients in β , γ and HCP-Mg phases. Hence, it is evident that the activation energies determined from the layer growth constants should not be the same as the activation energy for interdiffusion within the phase itself. This justifies the difference between the activation energies for the growth of the β and γ phases reported in Table 3 and that for interdiffusion within these phases reported in Tables 6 and 7.

Table 9 presents the activation energies of growth of the β and γ phases estimated in the present study compared with two previous studies reported by Funamizu et al.^[9] and Brubaker et al.^[10] The estimated values for the β phase significantly differ from each other. The activation energy for the growth of the γ phase reported in this study agrees well with that estimated from the data reported by Brubaker et al. but differs from that reported by Funamizu et al. It should be noted that Brubaker et al. have estimated the layer growth constants for temperature range of 360-420 °C from one diffusion couple experiments at each temperature. Thus, they have estimated the layer growth constants based on the equation $h^2 = kt$, which does not account for the incubation time required for nucleation of a phase. However, in the present study, the layer width data at three different temperatures are fitted to Eq 6, which does account for the incubation time. Not accounting for incubation time leads to lower-than-actual estimates of the layer growth constants, which in turn leads to higher estimates of activation energies. It is clear from Table 2 that the β phase has long incubation times, especially at temperatures of 400 °C and below. Hence, it is not surprising that the value of activation energy for the growth of the β phase estimated from the data of Brubaker et al. is higher than that found in the present study. The γ phase however has very short incubation times and hence, the activation energies from the two studies are very close to each other.

Funamizu et al. have also determined the activation energies for the growth of the β and γ phases from diffusion couple experiments for multiple times at each temperature. Still, the activation energies reported by them do not match with our estimates. A possible reason for the difference in the two data maybe the experimental procedure employed by Funamizu et al. for their diffusion couple experiments. They have reported that the diffusion couples were welded at 400 °C for 15 min before the actual isothermal diffusion annealing at selected temperatures. It can be seen from Table 2 that the incubation time of the γ phase at 400 °C is lower than that of β phase. Thus, the diffusion couple experiments of Funamizu et al. may have possibly started with some γ -nuclei already present in the couple. This will affect the phase growth kinetics especially at temperatures below 400 °C and most of the temperatures studied by Funamizu et al. are below 400 °C. This is supported by the lower activation energy for the growth of the γ phase found by Funamizu et al. than observed in the present study. It should also be noted that Funamizu et al. did not observe the presence of the ϵ phase in their diffusion couples in the entire range of temperatures studied, which also includes 325, 335 and 365 °C. However, the existence of the ϵ phase layer in a diffusion couple below \sim 370 °C has been confirmed by various studies.^[6,9] It is possible that in

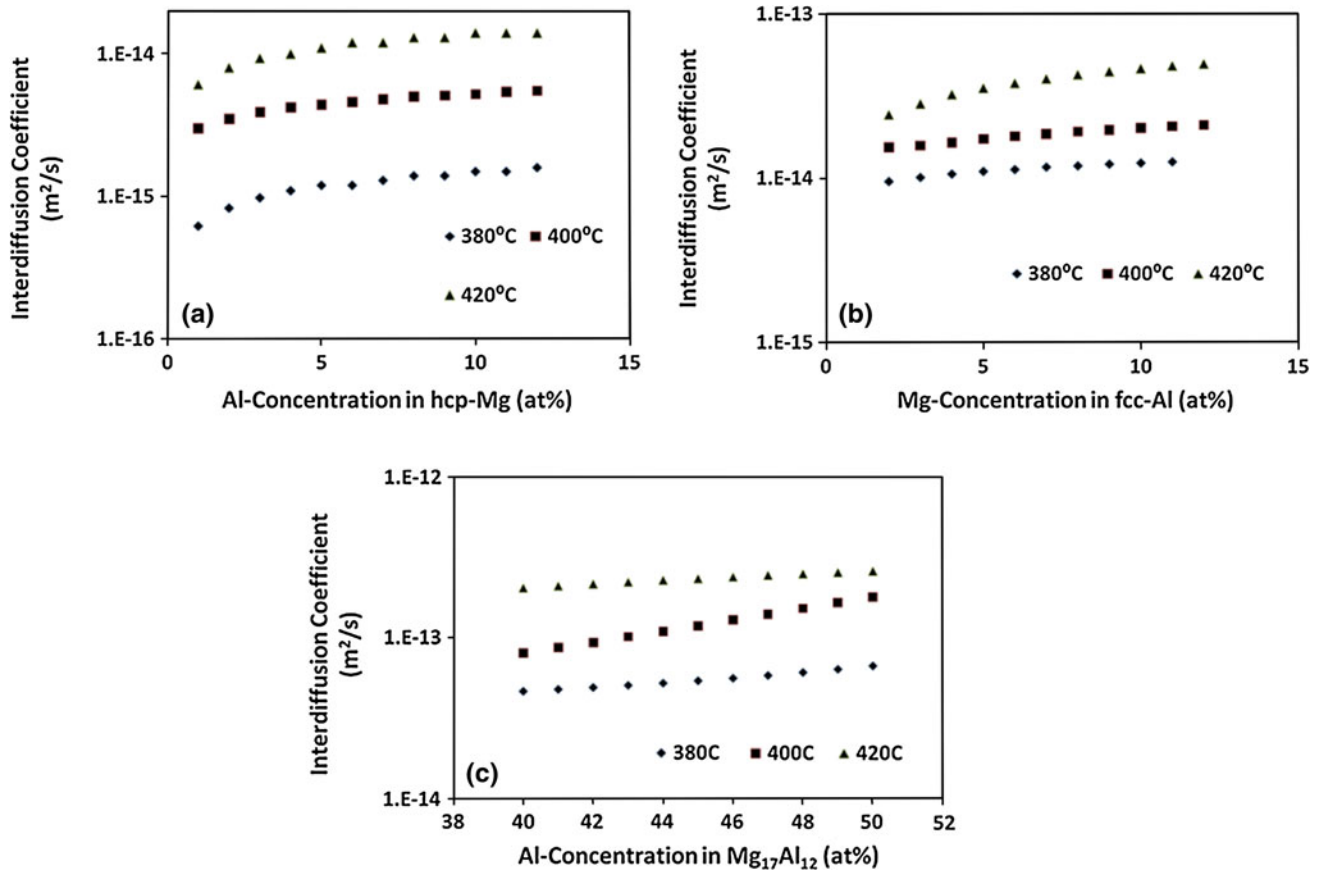


Fig. 8 Interdiffusion coefficients as functions of composition in (a) HCP-Mg, (b) FCC-Al, and (c) $\gamma\text{-Mg}_{17}\text{Al}_{12}$

Table 4 Interdiffusion coefficients as functions of composition in HCP-Mg

at.% Al	Interdiffusion coefficient \tilde{D} (m^2/s)			\tilde{Q} , kJ/mol	\tilde{D}_0 , m^2/s
	380 °C	400 °C	420 °C		
1	6.2×10^{-16}	3.0×10^{-15}	6.1×10^{-15}	215.8 ± 8.6	$129.0 (+28.6/-23.4)$
2	8.3×10^{-16}	3.5×10^{-15}	8.0×10^{-15}	213.6 ± 4.3	$111.1 (+11.0/-10.0)$
3	9.8×10^{-16}	3.9×10^{-15}	9.3×10^{-15}	212.1 ± 4.2	$96.5 (+9.1/-8.3)$
4	1.1×10^{-15}	4.2×10^{-15}	1.0×10^{-14}	208.0 ± 4.2	$50.9 (+4.1/-3.8)$
5	1.2×10^{-15}	4.4×10^{-15}	1.1×10^{-14}	208.7 ± 2.1	$62.2 (+2.5/-2.4)$
6	1.2×10^{-15}	4.6×10^{-15}	1.2×10^{-14}	216.9 ± 2.2	$281.5 (+17.4/-16.4)$
7	1.3×10^{-15}	4.8×10^{-15}	1.2×10^{-14}	209.3 ± 2.1	$75.9 (+3.1/-2.9)$
8	1.4×10^{-15}	5.0×10^{-15}	1.3×10^{-14}	209.8 ± 2.1	$89.1 (+4.1/-3.9)$
9	1.4×10^{-15}	5.1×10^{-15}	1.3×10^{-14}	209.9 ± 2.1	$90.0 (+4.2/-4.0)$
10	1.5×10^{-15}	5.2×10^{-15}	1.4×10^{-14}	210.3 ± 2.1	$102.5 (+4.8/-4.0)$
11	1.5×10^{-15}	5.4×10^{-15}	1.4×10^{-14}	210.3 ± 2.1	$104.6 (+5.0/-4.8)$
12	1.6×10^{-15}	5.5×10^{-15}	1.4×10^{-14}	204.2 ± 2.0	$36.2 (\pm 1.3)$

Funamizu's experiments, the presence of nuclei occurring from 400 °C weld treatment maybe affecting the nucleation and growth kinetics of the ϵ as well as the β phase in the diffusion couples studied at temperatures lower than 400 °C. However, in our experiments, no such pre-weld treatment has been employed and hence the growth kinetics data in each couple precisely correspond to the reported diffusion annealing temperature of the couple.

5.2 Interdiffusion Coefficients

There have been some interdiffusion data in Mg-Al system reported in the literature.^[7-9] However, there is a lack of data on interdiffusion coefficients in Mg-Al system evaluated as functions of composition; which was one of the main objectives of this work. The interdiffusion coefficients evaluated in the present study in various phases at 380, 400 and 420 °C as well

Table 5 Interdiffusion coefficients as functions of composition in FCC-Al

at.% Mg	Interdiffusion coefficient \tilde{D} , m ² /s			\tilde{Q} , kJ/mol	\tilde{D}_0 , m ² /s
	380 °C	400 °C	420 °C		
2	9.5×10^{-15}	1.5×10^{-14}	2.4×10^{-14}	88.4 ± 0.9	$1.1 (\pm 0.2) \times 10^{-7}$
3	1.0×10^{-14}	1.6×10^{-14}	2.8×10^{-14}	97.1 ± 1.0	$5.7 (+0.9/-0.7) \times 10^{-7}$
4	1.1×10^{-14}	1.7×10^{-14}	3.2×10^{-14}	104.8 ± 1.1	$2.5 (+0.7/-0.6) \times 10^{-6}$
5	1.1×10^{-14}	1.7×10^{-14}	3.5×10^{-14}	109.7 ± 3.3	$6.2 (+2.7/-1.3) \times 10^{-6}$
6	1.1×10^{-14}	1.8×10^{-14}	3.8×10^{-14}	113.5 ± 3.4	$1.3 (+0.5/-0.4) \times 10^{-5}$
7	1.2×10^{-14}	1.9×10^{-14}	4.0×10^{-14}	116.0 ± 3.5	$2.1 (+0.8/-0.6) \times 10^{-5}$
8	1.2×10^{-14}	1.9×10^{-14}	4.3×10^{-14}	119.8 ± 3.6	$4.3 (+1.5/-1.1) \times 10^{-5}$
9	1.2×10^{-14}	2.0×10^{-14}	4.5×10^{-14}	121.6 ± 3.6	$6.1 (+2.1/-1.5) \times 10^{-5}$
10	1.2×10^{-14}	2.0×10^{-14}	4.7×10^{-14}	124.0 ± 4.9	$9.6 (+3.1/-2.3) \times 10^{-5}$
11	1.3×10^{-14}	2.1×10^{-14}	4.8×10^{-14}	126.0 ± 3.8	$1.4 (0.4/-0.3) \times 10^{-4}$

Table 6 Interdiffusion coefficients as functions of composition in γ -Mg₁₇Al₁₂

at.% Al	Interdiffusion coefficient \tilde{D} , m ² /s			\tilde{Q} , kJ/mol	\tilde{D}_0 , m ² /s
	380 °C	400 °C	420 °C		
40	4.7×10^{-14}	8.1×10^{-14}	2.1×10^{-13}	138.3 ± 4.2	$5.1 (+0.9/-0.7) \times 10^{-3}$
41	4.8×10^{-14}	8.7×10^{-14}	2.1×10^{-13}	138.6 ± 2.8	$5.6 (\pm 0.6) \times 10^{-3}$
42	5.0×10^{-14}	9.4×10^{-14}	2.2×10^{-13}	138.8 ± 1.4	$6.0 (\pm 0.3) \times 10^{-3}$
43	5.1×10^{-14}	1.0×10^{-13}	2.2×10^{-13}	138.6 ± 1.4	$6.2 (\pm 0.3) \times 10^{-3}$
44	5.3×10^{-14}	1.1×10^{-13}	2.3×10^{-13}	138.3 ± 1.4	$6.1 (\pm 0.3) \times 10^{-3}$
45	5.4×10^{-14}	1.2×10^{-13}	2.3×10^{-13}	137.3 ± 1.4	$5.3 (\pm 0.3) \times 10^{-3}$
46	5.6×10^{-14}	1.3×10^{-13}	2.4×10^{-13}	136.4 ± 1.4	$4.7 (+0.3/-0.2) \times 10^{-3}$
47	5.9×10^{-14}	1.4×10^{-13}	2.5×10^{-13}	135.2 ± 2.7	$4.0 (+0.5/-0.4) \times 10^{-3}$
48	6.1×10^{-14}	1.5×10^{-13}	2.5×10^{-13}	133.1 ± 4.0	$2.9 (\pm 0.5) \times 10^{-3}$
49	6.4×10^{-14}	1.7×10^{-13}	2.6×10^{-13}	130.8 ± 5.2	$2.0 (+0.6/-0.4) \times 10^{-3}$
50	6.7×10^{-14}	1.8×10^{-13}	2.6×10^{-13}	128.3 ± 7.7	$1.4 (+0.7/-0.4) \times 10^{-3}$

Table 7 Average interdiffusion coefficients in β -Al₃Mg₂

at.% Al	Interdiffusion coefficient \tilde{D} , m ² /s			\tilde{Q} , kJ/mol	\tilde{D}_0 , m ² /s
	380 °C	400 °C	420 °C		
36-39	1.8×10^{-12}	2.4×10^{-12}	2.8×10^{-12}	44 ± 1.8	$5.9 (+6.7/-3.2) \times 10^{-9}$

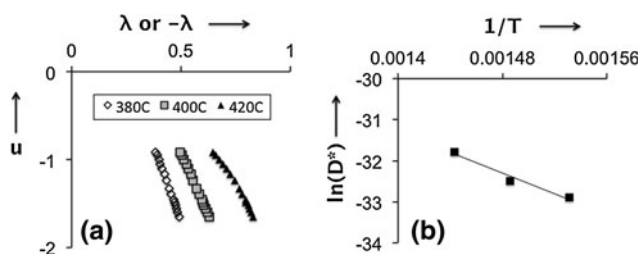


Fig. 9 (a) Plots of u vs. λ determined for Mg in FCC-Al region from the concentration profiles presented in Fig. 5, 6, 7. Note that x -axis represents λ for 400 and 420 °C data and $-\lambda$ for 380 °C data. (b) Arrhenius plot for Impurity diffusion coefficients of Mg in FCC-Al determined at 380, 400 and 420 °C

as the activation energies for interdiffusion in HCP-Mg, FCC-Al, γ and β phases are presented in Tables 4, 5, 6, 7.

The interdiffusion coefficients in HCP-Mg increase with increasing Al-content, Fig. 8(a); and that in FCC-Al increase slightly with increasing Mg-content, Fig. 8(b). Table 4 shows that the activation energy for interdiffusion in HCP-Mg does not show any particular trend with composition. It can be seen from Table 5 that the activation energy for interdiffusion in FCC-Al increases with increasing Mg-content. The effect of increased Mg-content on interdiffusion in FCC-Al maybe possibly explained based on the relative atomic sizes of Al and Mg. Atomic radii of Al and Mg are 0.143 and 0.160 nm respectively. Thus, Mg-atoms are about 12% larger than Al atoms, which means the FCC

Table 8 Activation energy and frequency factor for the impurity diffusion of Mg in FCC-Al

Parameter	Reported by Rothman et al. ^[23]	Reported by Hirano et al. ^[24]	Observed in Present Work
Activation energy, kJ/mol	130	114.7 ± 1	105.4 ± 4.2
Frequency factor	1.2 × 10 ⁻⁴	6.23 (+1.3/-1.0) × 10 ⁻⁶	1.33 (+1/-0.5) × 10 ⁻⁶

Table 9 Activation energy for the growth of β and γ phases as reported in various studies

Phase	Activation energy, kJ/mol		
	Reported by Funamizu et al. ^[9]	Estimated from data of Brubaker et al. ^[10]	Observed in present work
β	62.8 ± 2.1	83.2 ± 10.8	37.3 ± 4.1
γ	143.7 ± 1.7	185.9 ± 7.4	187.7 ± 1.9

Table 10 Interdiffusion coefficients in β and γ phases at 425 °C reported in various studies

Phase	Interdiffusion coefficient, m ² /s			
	Reported by Heumann ^[7]	Reported by Funamizu by Heumann's method ^[9]	Reported by Funamizu by Kidson's method ^[9]	Estimated from present work at average composition of the phase
β	1.7 × 10 ⁻¹²	1.4 × 10 ⁻¹²	1.1 × 10 ⁻¹²	3 × 10 ⁻¹²
γ	2.1 × 10 ⁻¹³	1.5 × 10 ⁻¹³	1.2 × 10 ⁻¹³	3 × 10 ⁻¹³

Al lattice is strained when a Mg-atom substitutes an Al atom. The increasing Mg content would lead to increased strain in the lattice, which in turn would lead to an increase in activation energy for atomic migration. Thus, the activation energy for interdiffusion in FCC Al-Mg alloy should increase with increasing Mg-content. On the other hand, substitution of larger Mg-atom by smaller Al atom in an HCP-Mg should not affect much the activation energy of atomic migration; thus, no specific trend in activation energy for interdiffusion with Al-content is expected in HCP-Mg.

Heumann and Kottman^[7] reported interdiffusion coefficients in the β and γ phases. Assuming linear variation of composition within a given intermediate phase, they derived the following equation for interdiffusion coefficient \tilde{D}_i assumed constant within the phase:

$$\tilde{D}_i = -\frac{W_i}{2t \cdot \Delta C_i} \int_0^{C_i^{1/2}} x dc_i, \quad (\text{Eq 12})$$

where W_i is the layer width of intermediate phase i , ΔC_i is the concentration difference between the two ends of the phase, and $C_i^{1/2}$ is the average concentration within the phase. For the assumption of linear concentration profile within a phase, the concentration gradient is simply given by $\Delta C_i/W_i$. Thus, it is clear that Eq 12 is just a combination of Eq 1 and 2 with the integral in Eq 12 giving the interdiffusion flux at the plane in the phase with the average concentration ($C_i^{1/2}$). Thus, Heumann's method in effect calculates the interdiffusion coefficient at the plane identified by average composition within the phase. Funamizu et al.^[9] have also used Heumann's method to calculate

interdiffusion coefficients in their Mg/Al diffusion couples. Funamizu has also used another approach, to calculate interdiffusion coefficients using Kidson's equation.^[28] In this approach, the interdiffusion coefficients assumed constant within each intermediate phase are calculated based on mass balance at the interface expressed as follows:

$$W_j = 2\sqrt{t} \left[\frac{(\tilde{D}K)_{j+1,j} - (\tilde{D}K)_{j,j+1}}{C_{j,j+1} - C_{j+1,j}} - \frac{(\tilde{D}K)_{j,j-1} - (\tilde{D}K)_{j-1,j}}{C_{j-1,j} - C_{j,j-1}} \right], \quad (\text{Eq 13})$$

where $K_{j,j+1}$ is $\sqrt{t} \cdot (dc/dx)_{j,j+1}$ and the suffix $j, j+1$ indicates the term in the j th phase at the interface between j and $j+1$ phases. Funamizu solved the simultaneous equations for interdiffusion coefficients in the two intermetallic phases, based on Eq 13 constructed at the three interfaces with the assumption of constant interdiffusion coefficient in each phase. It can be easily seen that Eq 13 can be obtained by integration of Eq 11 for constant interdiffusion coefficients.

Table 10 summarizes the interdiffusion coefficients obtained in the β and γ phases at 425 °C by Heumann and Kottman, and by Funamizu based on Heumann's and Kidson's methods. These are also compared with the interdiffusion coefficients calculated from present work at 425 °C at the average composition planes in the β and γ phases. There is a fair agreement between all the results. It should be noted that Heumann's method requires determination of Matano plane as a reference plane and hence, involves errors related to calculation of Matano planes, the position of which also differ for the two components in a multiphase couple. However, the method used in this study

based on Eq 4 is free of errors related to the Matano plane determination.

Kim et al.^[29] have simulated the concentration profiles and phase growth in a diffusion couple assembled between pure Mg and pure Al. Their model is based upon the interdiffusion coefficient (\tilde{D}) values assumed constant within each phase. The data reported by Kim et al. can be compared at a common temperature of 420 °C. At this temperature for 10 days, they have reported the thicknesses of β -Al₃Mg₂ and γ -Mg₁₇Al₁₂ layers to be respectively 497 and 261 μm . The layer thicknesses estimated based upon present study are about 622 and 341 μm respectively. The difference can be understood based upon the lower values of \tilde{D} used by Kim et al. for their simulations. The \tilde{D} values evaluated based upon the data used by Kim et al. for HCP-Mg, FCC-Al, β -Al₃Mg₂ and γ -Mg₁₇Al₁₂ are 5.4×10^{-15} , 4×10^{-15} , 1.6×10^{-12} and 1.1×10^{-13} m²/s respectively whereas the average values of \tilde{D} determined at 420 °C from the present study are 1.1×10^{-14} , 3.7×10^{-14} , 2.8×10^{-12} and 2.3×10^{-13} m²/s, respectively.

5.3 Impurity Diffusion of Mg in FCC-Al:

As can be seen from Table 8, the activation energy for the impurity diffusion of Mg in FCC-Al as determined by Hall's technique is found to be 105.4 ± 4.2 kJ/mol whereas the frequency factor is found to be $1.3 (+1.0/-0.5) \times 10^{-6}$ m²/s. Tracer technique is the most accurate technique for experimental determination of impurity diffusion. There have been two experimental studies reported in literature that determined the impurity diffusion of Mg in Al by tracer technique. Rothmann et al.^[23] studied the tracer diffusion of Mg in Al single crystals in the temperature range of 394-655 °C and Hirano et al.^[24] studied the impurity diffusion of Mg in polycrystalline Al in the temperature range of 325-650 °C. It should be noted here that the present study also estimates the impurity diffusion of Mg in polycrystalline Al and the temperature range studied here lies entirely within that studied by Hirano et al. It can be seen from Table 8 that the impurity diffusion parameters determined in the present study are fairly close to the data reported by Hirano et al.

6. Conclusions

1. Two intermediate intermetallic layers viz. Al₃Mg₂ (β) and Mg₁₇Al₁₂ (γ) were formed in the diffusion couple between pure Mg and pure Al at temperatures of 380, 400 and 420 °C.
2. The β -phase was observed to be growing considerably faster than γ -phase at all temperatures, and both phases grew parabolically with time i.e. the layer thickness was proportional to the square root of time. The parabolic growth suggests that the growth of both the phases is controlled by diffusion mechanisms.
3. The activation energies for the growth of the β and γ phases determined from the layer growth constants were found to be 37.3 (± 4.1) and 187.7 (± 1.9) kJ/mol, respectively in the temperature range of 380-420 °C.

4. The interdiffusion coefficients and activation energies for interdiffusion were evaluated as functions of compositions in the temperature range of 380-420 °C. Boltzmann-Matano analysis was utilized to evaluate the interdiffusion coefficients as functions of composition in all the four phases occurred in the diffusion couples viz. HCP-Mg, FCC-Al, β and γ . The activation energy for interdiffusion in FCC-Al increases with increasing Mg-content whereas no specific trend was observed in the activation energy for interdiffusion in HCP-Mg and γ -phase with the composition. The average values of the activation energies for interdiffusion in HCP-Mg (1-12 at.% Al), FCC-Al (2-11 at.% Mg), Mg₁₇Al₁₂ (40-50 at.% Al) and Al₃Mg₂ (36-39 at.% Al) are 210.7 ± 3.5 , 112.1 ± 12.2 , 135.8 ± 3.6 and 44 ± 1.8 kJ/mol respectively.
5. The activation energy and frequency factor for impurity diffusion of Mg in FCC-Al determined based on Hall's method are found to be 105.4 ± 4.2 kJ/mol and $1.3 (+1.0/-0.5) \times 10^{-6}$ m²/s respectively, in the temperature range studied.

Acknowledgment

The authors wish to acknowledge Krishnamoorthy R., Kiran Rao, Subramaniam and Manjunath K. for their laboratory support. Dr. Arun Kumar and Dr. Anil Sachdev are greatly appreciated for the useful technical discussions with the authors and also for reviewing the manuscript. Great thanks to Prof. Vikram Jayaram, Prof. Alope Paul, Dr. Ravi and Ms. Vandana Kulkarni for facilitating the use of EPMA at Indian Institute of Science, Bangalore. Professor Dayananda from Purdue University is acknowledged for useful technical discussions with authors. Finally, the authors also thank the management of GM for supporting this research.

References

1. K. Kulekci, Magnesium and Its Alloys Applications in Automotive Industry, *Int. J. Adv. Manuf. Technol.*, 2008, **39**, p 851-865
2. A.A. Luo and A.K. Sachdev, Microstructure and Mechanical Properties of Mg-Al-Mn and Mg-Al-Sn Alloys, *Magnesium Technology 2009*, E.A. Nyberg et al., Ed., TMS, Warrendale, PA, 2009, p. 437-443
3. F. Casarotto, A.J. Franke, and R. Franke, Chapter 6: High-Pressure Die-Cast (hpdc) Aluminium Alloys for Automotive Applications, *Advanced Materials in Automotive Engineering*, Woodhead Publishing Ltd., Cambridge, 2012, p. 109-149
4. A.A. Luo, Recent Magnesium Alloy Development for Elevated Temperature Applications, *Int. Mater. Rev.*, 2009, **49**, p 13-30
5. E. Aghion, B. Bronfin, F. Von Buch, S. Schumann, and H. Friedrich, Newly Developed Magnesium Alloys for Powertrain Applications, *JOM*, 2003, **55**, p 30-33
6. J.B. Clark and F.N. Rhines, Aluminum-Magnesium Equilibrium Diagram, *Trans. AIME*, 1957, **209**, p 6-7

7. Th. Heumann and A. Kottmann, Über den Ablauf der Diffusionsvorgänge in Substitutionsmischkristallen, *Z. Metallk.*, 1953, **44**, p 139-154
8. G. Moreau, J.A. Cornet, and D. Calais, Acceleration de La Diffusion Chimique Sous Irradiation Dans Le Systeme Aluminium-Magnesium, *J. Nucl. Mater.*, 1971, **38**, p 197-202
9. Y. Funamizu and K. Watanabe, Interdiffusion in the Al-Mg System, *Trans. Jap. Inst. Met.*, 1972, **13**, p 278-283
10. C. Brubaker and Z.-K. Liu, Diffusion Couple Study of Mg-Al System, *Magnesium Technology 2004*, A. Luo, Ed., TMS, Warrendale, PA, 2004, p. 229-234
11. J.-O. Andersson, T. Helander, L. Hoglund, P. Shi, and B. Sundman, THERMO-CALC & DICTRA, Computational Tools For Materials Science, *CALPHAD*, 2002, **26**(2), p 273-312
12. W. Cao, S.-L. Chen, F. Zhang, K. Wu, Y. Yang, Y.A. Chang, R. Schmid-Fetzer, and W.A. Oates, PANDAT Software with PanEngine, PanOptimizer and PanPrecipitation for Multi-Component Phase Diagram Calculation and Materials Property Simulation, *CALPHAD*, 2009, **33**, p 328-342
13. A. Fick, On Liquid Diffusion, *Poggendorff's Ann. Phys.*, 1855, **94**, p 59
14. M.A. Dayananda and C.W. Kim, Zero-Flux Planes and Flux Reversals in Cu-Ni-Zn Diffusion Couples, *Metall. Trans. A*, 1979, **10**(9), p 1333-1339
15. M.A. Dayananda, An Analysis of Concentration Profiles for Fluxes, Diffusion Depths, and Zero-Flux Planes in Multicomponent Diffusion, *Metall. Trans. A*, 1983, **14A**(9), p 1851-1858
16. G.H. Cheng and M.A. Dayananda, Multiphase Diffusion in Fe-Ni-Al System at 1000 °C: II. Interdiffusion Coefficients for Beta and Gamma Alloys, *Metall. Trans. A*, 1979, **10A**(10), p 1415-1419
17. P.C. Tortorici and M.A. Dayananda, Growth of Silicides and Interdiffusion in the Mo-Si System, *Metall. Trans. A*, 1999, **30A**, p 545-550
18. P.C. Tortorici and M.A. Dayananda, Diffusion Structures in Mo Versus Si Solid-Solid Diffusion Couples, *Scr. Mater.*, 1998, **38**(12), p 1863-1869
19. L.D. Hall, An Analytical Method of Calculating Variable Diffusion Coefficients, *J. Chem. Phys.*, 1953, **21**(1), p 87-89
20. J.L. Murray, The Al-Mg (Aluminum-Magnesium) System, *Bull. Alloy Phase Diagr.*, 1982, **3**, p 60-74
21. T.B. Massalski, Ed., *Binary Alloy Phase Diagrams*, ASM International, Materials Park, OH, 1990
22. M.A. Dayananda and L.R. Ram-Mohan, *MultiDiffux*, Purdue University, West Lafayette, 2005
23. S.J. Rothman, N.L. Peterson, L.J. Nowicki, and L.C. Robinson, Tracer Diffusion of Magnesium in Aluminum Single Crystals, *Phys. Stat. Solidi B*, 1974, **63**, p K29-K33
24. K. Hirano and S. Fujikawa, Impurity Diffusion in Aluminum, *J. Nucl. Mater.*, 1978, **69/70**, p 564-566
25. Y. Zuo and Y.A. Chang, Thermodynamic Calculation of the Al-Mg Phase Diagram, *CALPHAD*, 1993, **17**(2), p 161-174
26. H.L. Su, M. Harmelin, P. Donnadieu, C. Baetzner, H.J. Siefert, H.L. Lukas, G. Effenberg, and F. Aldinger, Experimental Investigations of the Mg-Al Phase Diagram from 47 to 63 at.% Al, *J. Alloy. Compd.*, 1997, **247**, p 57-65
27. R.D. Sisson and M.A. Dayananda, Diffusion Structures in Multiphase Cu-Ni-Zn Couples, *Metall. Trans. B*, 1972, **3**, p 647-652
28. G.V. Kidson, Some Aspects of Growth of Diffusion Layers in Binary Systems, *J. Nucl. Mater.*, 1961, **3**(1), p 21-29
29. Y.M. Kim, S.K. Das, M. Paliwal, and I.H. Jung, Multiphase Diffusion Study for Mg-Al Binary Alloy System, *Magnesium Technology 2011*, W. H. Sillekens et al., Ed., TMS, Warrendale, PA, 2011, p. 49-53